

Catalytic Conversion of Simulated Biogas Mixtures to Synthesis Gas in a Fluidized Bed Reactor Supported by a DBD

Thorsten Kroker · Torsten Kolb · Andreas Schenk ·
Krzysztof Krawczyk · Michal Młotek · Karl-Heinz Gericke

Received: 15 September 2011 / Accepted: 17 February 2012 / Published online: 7 March 2012
© Springer Science+Business Media, LLC 2012

Abstract The catalytic conversion of methane and carbon dioxide was studied in a fluidized bed reactor supported by a 13.56 Hz driven coaxial DBD-reactor. Palladium or copper catalyst which are covered on Al_2O_3 particles were used. The goal was to test whether biogas can be used for the production of synthesis gas. The influences of discharge power, catalysts and temperature of the catalyst bed on the product yield were studied. The starting material and product stream was analyzed by quadrupole mass spectrometry and infrared spectroscopy. H_2/CO ratios can be adjusted in a range between 0.65 (without a catalyst) and 1.75 (using a copper catalyst). The process is highly selective for hydrogen production (up to 83%, using a Palladium catalyst). A copper catalyst increases the H_2/CO ratio can from 1.04 to 1.16 and the palladium catalyst from 1.11 to 1.43 by heating the catalyst to a temperature of 250°C.

Keywords Biogas · Cold plasma · Fluidized bed reactor · Synthesis gas · Online monitoring

Introduction

Synthesis gas is a basis for many industrial processes [1]. Recently the greenhouse gases methane and carbon dioxide have been used as alternative starting material for the synthesis gas production. Conventional [2–4] as well as plasma assisted reactors were used for this way of synthesis gas production [5–17]. Biogas produced by putrefaction processes from rotting biomass is a major source of these two greenhouse gases with an average composition of 60% methane and 35% carbon dioxide. Using biogas or biomass as starting material for synthesis gas production is an excellent idea because it relies on an exhaustless

T. Kroker · T. Kolb · A. Schenk · K.-H. Gericke (✉)
Institute of Physical and Theoretical Chemistry, Hans Sommerstraße 10,
38106 Braunschweig, Germany
e-mail: k.gericke@tu-bs.de

K. Krawczyk · M. Młotek
Faculty of Chemistry, Warsaw University of Technology, 00-664 Warszawa, Poland

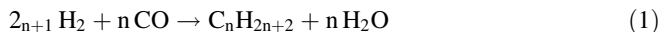
source of a renewable material [18–20]. The second big advantage is that biogas is very inexpensive. Last but not least getting rid of harmful greenhouse gases is another desired effect.

For industrial applications a continuous method, like the Plug-flow-reactor, is useful. In addition, online monitoring allows adjustment of the reactor configuration whenever necessary. Online monitoring is very helpful because Biogas composition is variable [21, 22]. Therefore, it is beneficial when the effect of these variations can be compensated for by changing the reactor conditions to obtain the desired product yield and selectivity.

Furthermore, catalysts allow optimization of the product distribution. Unwanted side effects are carbon deposition on the surface of the catalyst and poisoning by sulfur. The typical source of sulfur is hydrogen sulfide, which is found in small amounts in biogas. The catalyst is deactivated and has to be regenerated. In a fluidized bed reactor small amounts of the catalyst can be exchanged continuously without interruption of the reaction process.

In this study a homogenous DBD and a heterogeneous fluidized bed DBD Reactor are compared to each other. The influence of changing the discharge power on the H₂/CO ratio (synthesis gas) was studied for both DBD designs. Because of the importance of the catalyst temperature on the product distribution, a catalyst heater was added at the lower area of the DBD-Reactor. In this way the temperature of the catalyst can be increased and the influence of the catalyst temperature on the synthesis gas yield and ratio can be studied. This is necessary because some catalysts need high temperatures (>250°C) to range the highest activity. The secondary function of the catalyst heating system is to regenerate the catalyst at very high temperatures of several 100°C using added gases, like O₂.

The synthesis gas can be refined by the Fischer–Tropsch synthesis especially to synthetic fuel:



It is important to know the H₂/CO ratios, because usually a ratio of 1.7 is used. Pressure, temperature and catalyst determine the product yield.

Another example of the application of the synthesis gas is the production of alcohols, especially methanol:



This process needs a H₂/CO ratio of 2:1.

Another well known synthesis is Hydroformylation, for which a molar ratio of 1:1 is required.



The main aim of the project is to characterize the yield of synthesis gas quantitatively and search for conditions to optimize the selectivity and the product yield.

Experimental Procedure

The experiment (Fig. 1) was performed in a fluidized bed reactor supported by a 13.56 MHz dielectric barrier discharge [23]. The DBD reactor (Fig. 2) is made from a 150 mm long Duran glass-tube with 8 mm outer diameter and 5 mm inner diameter. The top of the reactor was extended with a Duran glass-ball with 20 mm diameter. The catalyst was laid on the bottom atop a piece of glass wool. The starting material gas stream disperses the catalyst

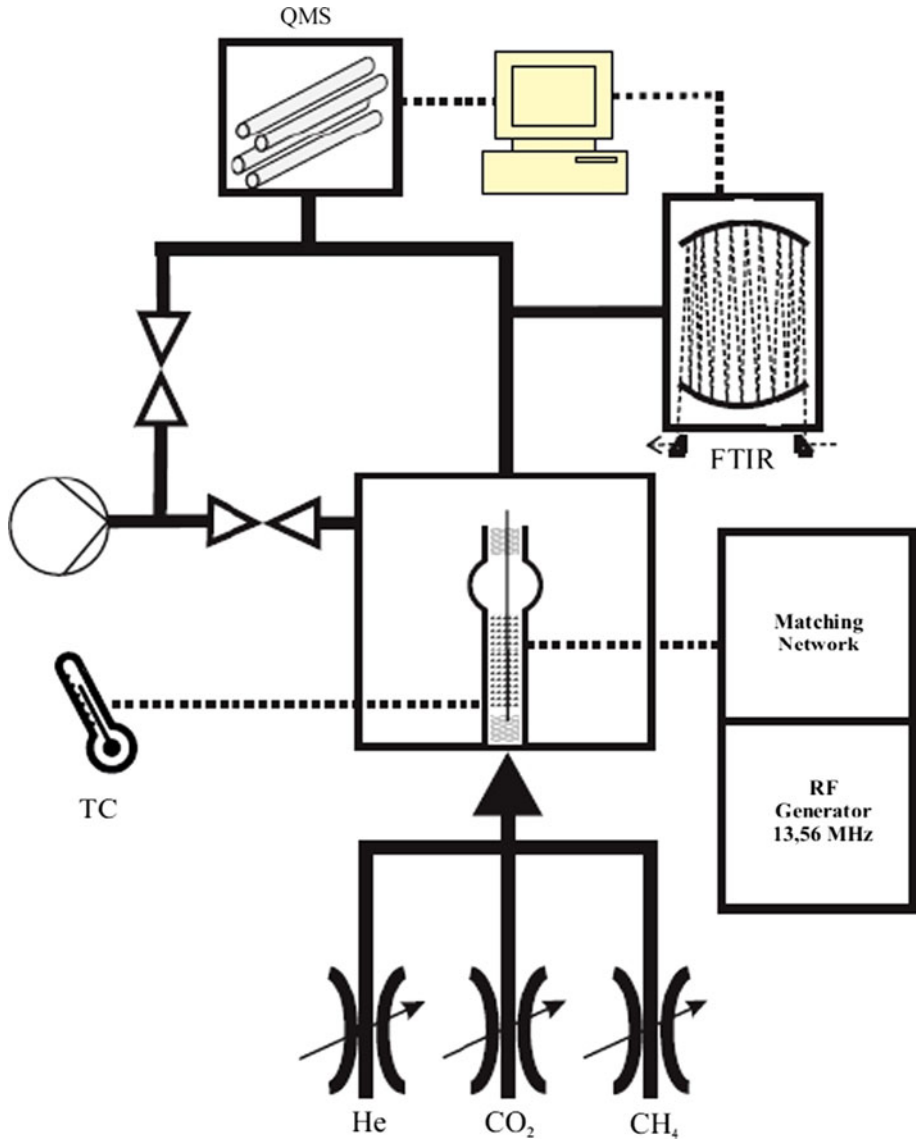


Fig. 1 Schematic setup of the gas flow system (*solid lines*) and electrical interfaces (*dashed lines*). The three MFCs (He, CO₂, CH₄) feed the experiment with the gases. *QMS* quadrupole mass spectrometer, *FTIR* FT-infrared spectrometer, *TC* thermo couple

and fluidizes it into the plasma zone. The catalyst expands into the glass-ball, where it slows down and trickles back to the bottom via the border of the reactor. Thus a closed loop is built.

Two portions of alumina-ceramic supported catalysts containing Cu and Pd (denominated as Cu/Al₂O₃, Pd/Al₂O₃ respectively) were prepared. The catalysts (each containing about 3 wt% of metal) were obtained by impregnation of alumina-ceramic particles of

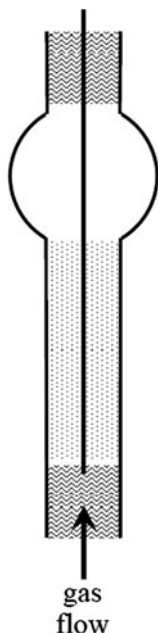


Fig. 2 Schematic picture of the reactor. *Dotted area* plasma/catalyst area, *shaded area* glass wool, *solid line* iron conductor

0.16–0.32 mm with aqueous solutions of $\text{Cu}(\text{NO}_3)_2$ and $\text{Pd}(\text{NO}_3)_4$, dried and calcined in ambient air at 400°C for 4 h. They were packed to the reactor without additional pre-treatment [24, 25].

The plasma was ignited over a length of 50 mm using silver paint and an iron conductor with a length of 100 mm and a diameter of 2 mm as electrodes.

The iron conductor was fixed by glass wool. This setup leads to residence times of 50 ms. The catalyst can be heated up to 250°C . The plasma was generated by a RF-generator (ENI ACG-6B) and an impedance controller (ENI MW-10D) at a frequency of 13.56 MHz. The discharge power can be adjusted directly on the RF-generator.

The pressure in the reactor chamber was kept constant at 100 mbar by a XDS dry pump (Edwards). A needle valve controls the gas flow and the pressure in the reaction chamber. The gases were adjusted by three mass flow controllers (MKS), at a total flow rate of 100 cm^3 per min. 3% CH_4 , 2% CO_2 and 95% Helium were used ($3/2/95\text{ cm}^3$ per min). The free electrons in the DBD reactor must have the ionization energy of the fed molecules to ignite the plasma. These electrons have a longer distance of acceleration to reach the energy if helium is used as a carrier, because its collision cross section is very small.

The products were analyzed online by FTIR-spectroscopy (Equinox 55, Bruker) in a White-cell with a path length of up to 4 m and a QMS (Balzer, QMS 200 Prisma). All data are measured with an accuracy of 1%. The temperature was measured with a thermo couple.

For the collection of carbon black data a DBD reactor equipped with a glass frit was built prevents that carbon black from exiting the reactor. Thus a quantitative detection of this product becomes possible. The reactor was run for 1 h for every discharge power step. Carbon black was produced for power higher than 40 W and was analyzed gravimetrically.

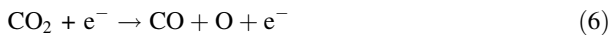
Results and Discussion

Reactions

Equation (4) describes the ideal transformation of methane and carbon dioxide to synthesis gas:



Synthesis gas formation mechanism is a very complex process. Here, only the most important reactions are described. The very first step is the generation of micro discharges in the reactor in which electrons with average energy between 1 and 10 eV induce the dissociation of methane and carbon dioxide. Equations (5) and (6) show the first steps in the chain mechanism of synthesis gas generation.



Equation (6) demonstrates that carbon monoxide can be produced in a simple reaction. However, for hydrogen production a second step is required. Equations (7) and (8) [26] are the two most probable mechanisms for hydrogen generation.



By successively removing more hydrogen from CH_x radicals the formation of carbon black becomes possible.



For a large hydrogen yield, implying a large H-radical concentration as well, a removal mechanism for CO can occur:



Calibration

Calibration of both product and starting material were performed in a direct way. A 10 cm^3 per min MFC was used to admix CO, H_2 (products), CH_4 or CO_2 (starting material) with helium. The method of calibration is demonstrated on the basis of CO. For the calibration of carbon monoxide 12 different gas mixtures were used. The first was 0.25 cm^3 per min CO and 99.75 cm^3 per min He (100 cm^3 per min total gas stream). In this way a mixing ratio was created with an amount of 0.25% CO. Afterward a FT-IR spectrum was measured. The flow of CO was increased in steps of 0.25 cm^3 per min and the He flow was accordingly decreased until the highest mixing ratio of 3.00 cm^3 per min CO and 97.00 cm^3 per min He was reached (3% CO).

The transmission of CO at 2,169 cm^{-1} (y-axis, see Fig. 3) was plotted over the mixing ratio of carbon monoxide (x-axis) and used for calibration with the fitting function:

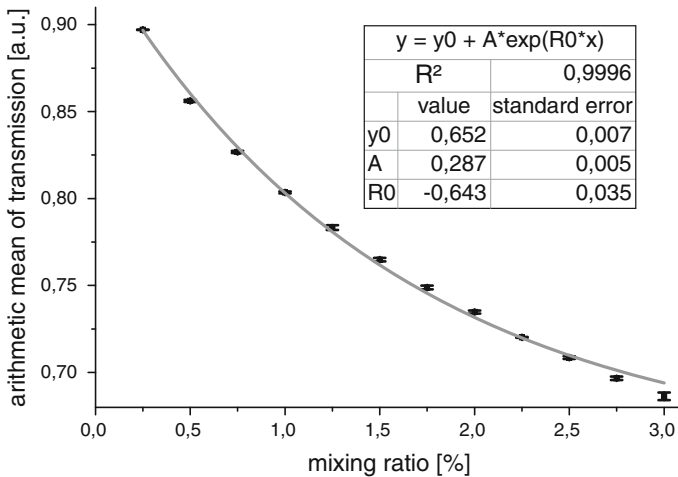


Fig. 3 Calibration curve of CO. The transmission of CO at $2,169 \text{ cm}^{-1}$ (y-axis) is plotted against mixing ratio of CO (x-axis). Y_0 , A and R_0 are fit parameters

$$y = y_0 + A \cdot \exp(R_0 \cdot x_{\text{CO}}) \quad (13)$$

The exponential part based on the Lambert–Beer law. R and A are fit parameters. Figure 3 shows the calibration curve for CO which was used in this experiment.

The non-zero interception of the y-axis (y_0) and the correspondingly small value of A are due to the instrumental bandwidth (1 cm^{-1}) of the FTIR spectrometer which significantly exceeds the spectral width due to the individual pressure boarded CO abs. line.

However, the correlation coefficient and the values of standard errors prove that the method used is very precise and the reproducibility is good.

Thereby the amount of CO generated in the plasma treated gas stream can be determined. Equation (13) can be transformed to

$$x_{\text{CO}} = \lg [(y - y_0)/A]/R_0 \quad (14)$$

to directly yield the amount of CO (based on a 100 cm^3 per min gas stream).

The same procedure was used for methane ($1,306 \text{ cm}^{-1}$) and carbon dioxide ($2,350 \text{ cm}^{-1}$). The amount of hydrogen was measured with the QMS and calculated with a linear approximation.

Catalyst Free DBD

Spectra were recorded in the range of $500\text{--}5,000 \text{ cm}^{-1}$, with a resolution of 1 cm^{-1} . Figure 4 shows an FTIR spectrum of a mixture of 3% methane, 2% carbon dioxide in helium with (product stream) and without plasma (starting material).

At first the starting material gas stream was analyzed and compared with the homogenous plasma treated gas stream (Fig. 4). Afterward the homogenous plasma result was compared with the heterogeneous plasma.

The selectivity of hydrogen was calculated from the conversion of methane (15) and the selectivity of carbon monoxide was calculated from the carbon balance of carbon dioxide and methane (16).

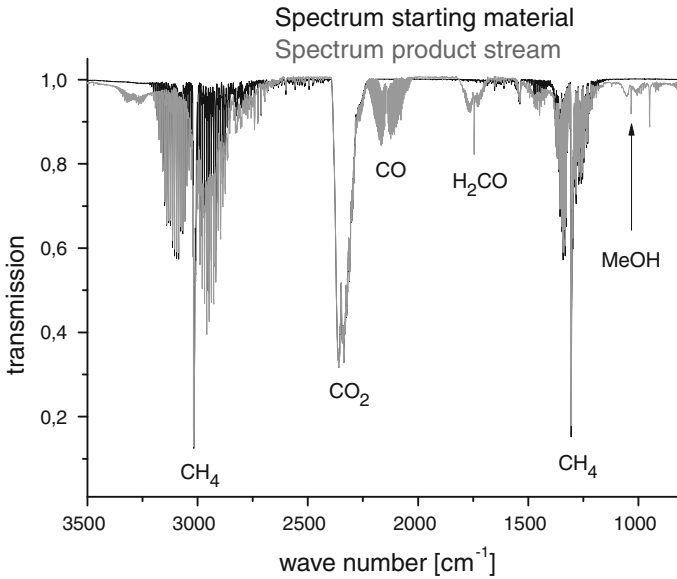


Fig. 4 Spectrum of starting material (3% CH₄ and 2% CO₂ in Helium) and product stream with a discharge power of 30 W

$$S(\text{H}_2) = 2 \cdot n_{\text{H}_2}(\text{H}_2) / 4 \cdot n_{\text{CH}_4}(\text{converted CH}_4) \tag{15}$$

$$S(\text{CO}) = 1 \cdot n_{\text{CO}}(\text{CO}) / 1 \cdot n_{\text{CH}_4}(\text{converted CH}_4) + 1 \cdot n_{\text{CO}_2}(\text{converted CO}_2) \tag{16}$$

S(H₂) and S(CO) are the selectivities of the products, n_x is the amount of the substance and the numbers before are the stoichiometric coefficients. As example, for methane the amount of the substance is given by (17)

$$n_{\text{CH}_4} = x_{\text{CH}_4} [\%] \cdot \text{con}_{\text{CH}_4} [\%] / 100 \tag{17}$$

x_{CH₄} is the amount of methane in the starting material (3%) and con_{CH₄} is the conversion of methane.

Figure 5 shows the detected amount of hydrogen and carbon monoxide (left y-coordinate) as well as H₂/CO ratio (right y-coordinate) as a function of plasma power. In contrast the left y-coordinate of Fig. 6 shows the conversion of methane and carbon dioxide as function of plasma power whereas the right y-coordinate shows the selectivity of hydrogen and carbon monoxide.

The yield of hydrogen in the product stream starts at 7% and increases up to 31.0%, while the yield of carbon monoxide was 10.8% at the lowest discharge power and increased up to 25% at the highest power (Fig. 5).

Therefore, at the lowest power the H₂/CO ratio is very small (0.7). It should be mentioned that at these low powers only a small number of micro discharges contribute to the plasma. The radicals (CH₃, H and O) of the two start reactions, (5) and (6), are only formed in small amounts. For formation of hydrogen a second step is needed (7 or 8), in contrast to the carbon monoxide which can be directly generated by (6). In this way a comparatively large amount of carbon monoxide can be formed in the product stream. The essential forming mechanism of hydrogen rather corresponds to (7), because the amount of hydrogen radicals is marginal and the chances that two hydrogen radicals collide is very

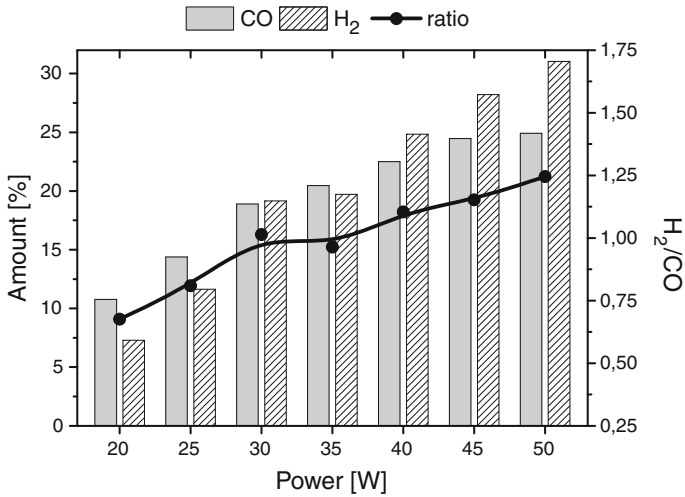


Fig. 5 Produced amount of H₂ and CO (left y-coordinate) and its ratio (right y-coordinate) without a catalyst. Temperature was between 40°C at 20 W and 80°C at 50 W discharge power (see Fig. 8)

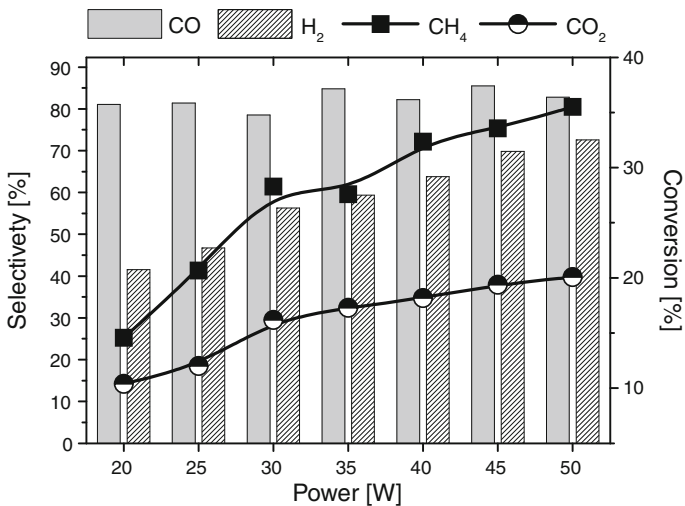


Fig. 6 Conversion and selectivity of CH₄ and CO₂ without a catalyst

small. Thus the second forming mechanism of hydrogen is almost disabled at lower power. This leads to small amounts of hydrogen. Reaction (12) is extensively disabled and leads to large amounts of carbon monoxide.

The ratio of H₂/CO increases with increasing energy (discharge power) up to 1.25. Similar results were reported by Guoa et al. [12]. The number of micro discharges increases significantly and the number of the radicals per volume increases, too. The reaction kinetics depend strongly on the concentration of the radicals. Therefore, the concentration of several intermediates is changed, resulting in different product yields. The second formation mechanism of hydrogen becomes more efficient and much more

hydrogen can be formed. When the number of micro discharges is very high the probability of collision of an electron with a radical like CH_3 . In this way a new hydrogen source comes into play (9–11) and the probability for decomposition of CO by H-radicals (12) is increased. On the other hand methane and carbon dioxide decompose with increasing plasma power and reaction (5) and (6) become less probable.

The conversion of methane is always higher than conversion of carbon dioxide, 15% for methane at 20 W and 10% for carbon dioxide (Fig. 5). The conversion efficiency of methane increases more quickly than the conversion of carbon dioxide with increasing power [20] because the dissociation energy of methane, 4.48 eV [27], is much lower than that of carbon dioxide, 5.52 eV [27]. At 50 W the conversion of methane is 31% compared to 25% for carbon dioxide. This demonstrates that the conversion strongly depends on electric power [5, 11, 12, 20]. Similar results can be observed at increased residence times [5, 11, 12, 20, 24].

The results for carbon monoxide indicate an essentially constant selectivity around 80%. It can be assumed that all converted carbon dioxide becomes carbon monoxide (6), as the elimination of the second oxygen atom of carbon dioxide can be essentially excluded, owing to the very high dissociation energy of carbon monoxide, 11.16 eV [27].

The assumption that conversion of carbon dioxide mainly produces carbon monoxide can be based on the selectivity of carbon monoxide. To explain such a high selectivity more than just mechanism 6 is needed. The carbon source for the production of carbon monoxide can be methane or carbon dioxide. We suggest a dehydrogenation mechanism of methane where all hydrogen atoms are converted to other products.

The selectivity of hydrogen increases significantly from 36 to 73% and is based on 15. These results are consistent with other results obtained in this project [23] and with results of other work groups [5, 11, 12]. The concentration of other hydrogen rich products like formaldehyde [23] is higher at lower discharge power. At the same time the selectivity of C_2 hydrocarbons, especially ethane, decreases with increasing plasma power [5, 11, 12].

Our results suggest a favored hydrogen formation at higher plasma power. The dissociation energy of hydrogen, 4.52 eV, is very similar to the dehydrogenation chain of methane. However, hydrogen is a very small molecule and, thus, the chance for the dissociation by electron impact is small. Very similar results can be obtained by changing the gas flow rate (and the residence time) [24].

The preference for hydrogen production agrees with the generation of a black solid, because it only occurs at higher plasma powers (Fig. 7). This solid which we call carbon black is not analyzed in detail. Only the generated amount of the black solid is for this experiment important not the composition, because too much carbon black destroys the catalyst. This experiment has only been done with the plug flow reactor. The results for fluidized bed reactor are expected to be the same but require much higher experimental efforts.

At powers less than 40 W no carbon black is observable. As soon as carbon black is produced, hydrogen can be formed with high selectivity. The source of carbon black is methane only, because no carbon black can be observed in a test series where carbon dioxide was used exclusively. When pure methane (without carbon dioxide) is used, we observe some carbon black, but not as much as when a combination of these two gases is used. The absence of carbon black in pure carbon dioxide plasma can be explained by the very stable carbon/oxygen bond.

Above 40 W the produced amount of carbon black follows an exponential trend (fitted line in Fig. 7 above 40 W). Therefore, we avoided investigating the plasma at higher

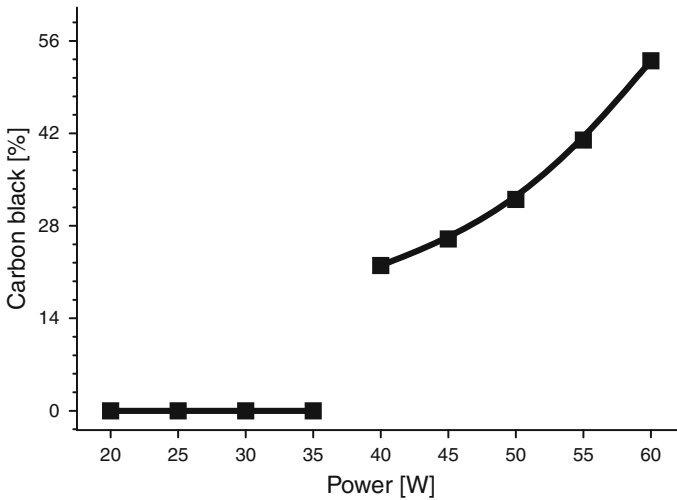
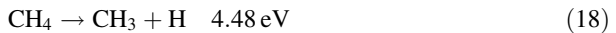


Fig. 7 Carbon Black production as function of plasma power

discharge powers than 50 W, because carbon black is very harmful for the catalyst and other parts of the setup, like the vacuum pump or the mirrors of the White-cell.

The generation of carbon black can be triggered in two ways. First it can be triggered by an excess of radicals and second by electrons that are emitted by the inner electrode. Such electrons can carry large energy once they have left the electrode initiating dehydrogenation of CH_x radicals and forming carbon black in this way. Additionally the populations of electrons per volume increase so that the start reactions as well as the dehydrogenation of methane to carbon black both become more probable. In contrast to carbon dioxide there is no significant increase in bond energy for successive dissociation.



In order to determine the influence of temperature on the product formation, the temperature of the reactor wall was measured by a thermo couple. Figure 8 shows the dependence of the temperature of the reactor wall as a function of the discharge power. As shown in Fig. 8 the temperature of the reactor rises only to 75–80°C at a discharge power of 50 W. Although the palladium is already active at lower temperatures [23], our results on external heating of the catalyst (chapter 3.4) indicate that the effect of external ohmic heating is insignificant within these measurements.

Fluidized Bed Reactor Supported by DBD

Using biogas for producing synthesis gas for processes like Fischer–Tropsch synthesis in a homogeneous system is rather inefficient. Therefore, a fluidized bed reactor for plasma assisted catalysis was built. The advantage of a fluidized bed reactor is that radicals and catalysts are in close contact and can react directly. In a packed bed reactor only the

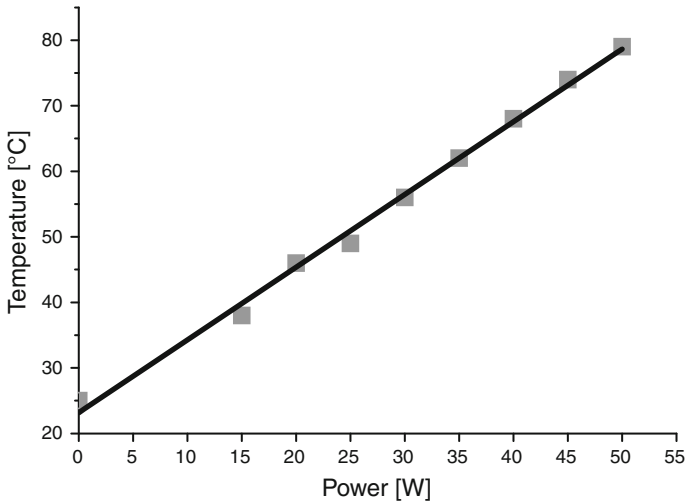


Fig. 8 Trend of temperature as function of discharge power

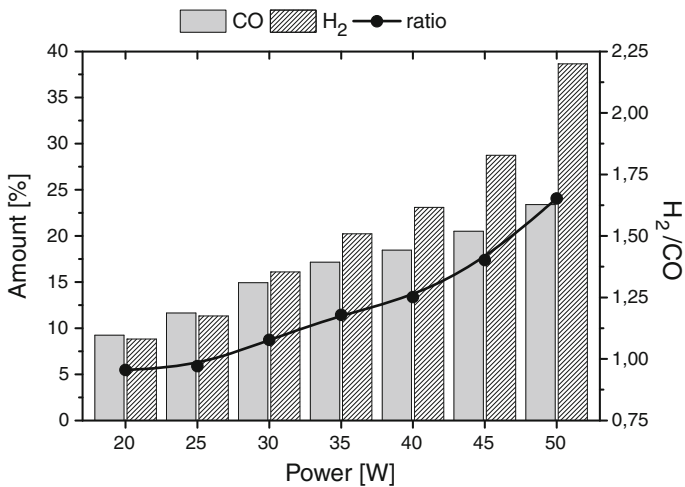


Fig. 9 Produced amount of H₂ and CO (left y-axis) and its ratio (right y-axis) with the Pd/Al₂O₃ catalyst

afterglow can react with the catalyst. The tested catalysts, Pd/Al₂O₃ and Cu/Al₂O₃, show very similar results at lower discharge power. As an example Figs. 9 and 10 show that the produced amounts of hydrogen and carbon monoxide are very similar. At lower discharge power (≤ 25 W) the synthesis gas ratio is 1.0 with the Pd/AlO_x and 1.1 with the Cu/AlO_x catalyst, in contrast to 0.7 without a catalyst (see Fig. 5). Thus, both catalysts increase the synthesis gas ratio. The highest H₂/CO ratio was found using the copper catalyst. With rising discharge power the H₂/CO ratio increases and at the highest power (limited by the production of carbon black) a ratio of 1.67 for the palladium catalyst (Fig. 9) and 1.7 for the copper catalyst (Fig. 10) was observed.

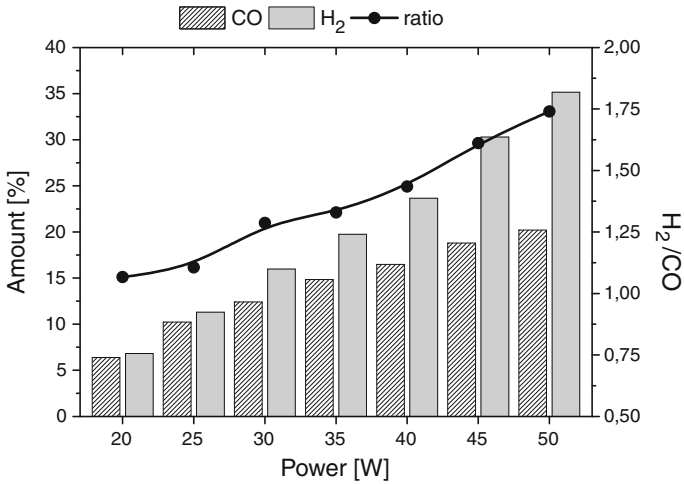


Fig. 10 Produced amount of H₂ and CO (left y-axis) and its ratio (right y-axis) with the Cu/Al₂O₃ catalyst

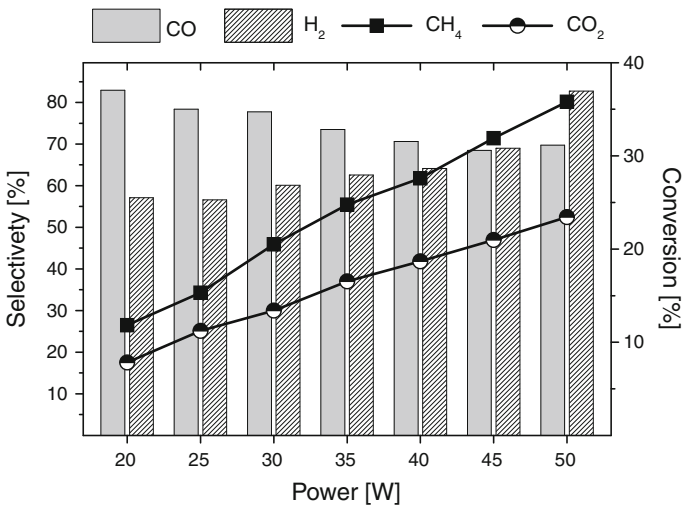


Fig. 11 Conversion of methane and carbon dioxide (left y-axis) and selectivity of the synthesis gas components (right y-axis) with the Pd/Al₂O₃ catalyst

Both catalysts increase the hydrogen yield significantly, and the Pd/AlOx catalyst produces the highest yield of hydrogen of 39% at 50 W, instead of 35% with the Cu/AlOx catalyst. Under catalyst free conditions the amount of hydrogen is 31% at 50 W. Both catalysts decrease the produced amount of carbon monoxide. Without a catalyst the amount of carbon monoxide was 25% at 50 W. The produced amount of carbon monoxide decreases to 23% with the fluidized Pd/AlOx catalyst and 20% with the Cu/AlOx catalyst. In this way much higher H₂/CO ratios can be obtained than under catalyst free conditions. Interestingly, the conversion of methane is more or less the same, but the conversion of carbon monoxide is much higher under fluidized bed conditions (see Figs. 6,11,12).

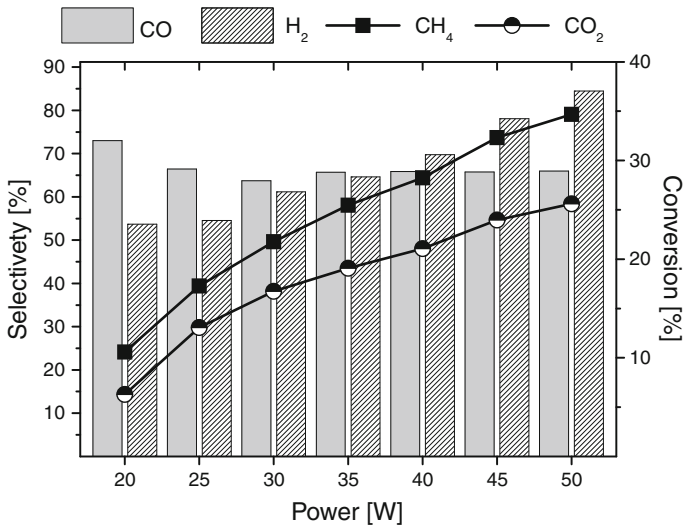


Fig. 12 Conversion of the starting material (*left y-axis*) and selectivity of hydrogen and carbon monoxide (*right y-axis*) with the Cu/Al₂O₃ catalyst

This result seems to be surprising, because the produced amount of CO should be increased with increasing CO₂ conversion (6). An explanation of this observation is the very high amount of hydrogen and consequently a high concentration of hydrogen radicals in the plasma. In this way a removal reaction of CO triggered by a high H-radical concentration, can be initiated according to (12). In addition, the catalyst can serve as energy acceptor (absorption of H-radicals) dominating the three-body-collision reaction. The CHO-radical can be converted to many other products [26]. Palladium can absorb hydrogen (chemisorption) in atomic form and in this manner accelerate H-radical reactions like (7), (8) and (12) or abstraction of hydrogen from CH_x radicals by H-radicals. The efficiency of chemisorption and solidity ratio strongly depends on temperature [28]. In the experiments reported here the temperature of the fluidized bed catalyst was only varied between 25 and 80°C (see Fig. 8). Chemisorption and solidity ratio are hardly influenced by such low temperatures. However, in order to study the effect of temperature, in another set of experiments the temperature of the fluidized bed was increased up to 250°C (see Chap. 3.5).

These results are consistent with the study of the ethane yield. The highest ethane concentration can be monitored using the copper catalyst while the lowest concentration is observed under catalyst free conditions. The ethane concentration is round about 1% and the selectivity for this reaction reaches values between 3 and 9%. For producing ethane much more carbon and hydrogen are needed, so these species are not available for other processes. The additional hydrogen consumption can be explained by the reduction of another hydrogen rich species like water.

The highest selectivity for hydrogen can be reached with the copper catalyst (85% at 50 W) instead of 83% with the Pd catalyst and 73% without a catalyst. The selectivity of hydrogen is based on the conversion of methane (15). Figure 13 summarizes the H₂/CO ratios.

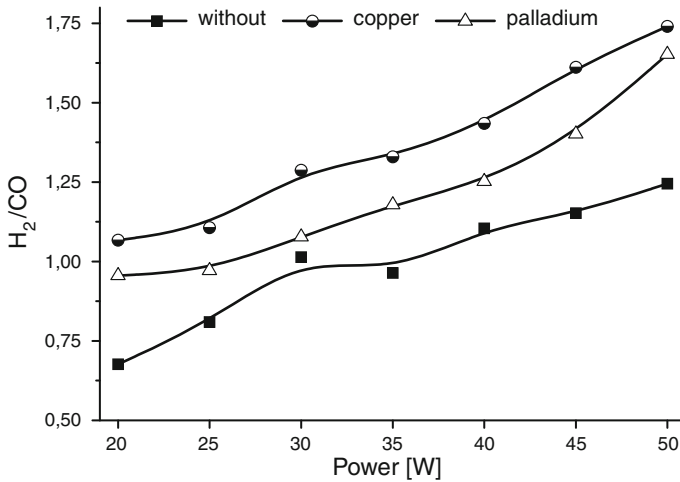


Fig. 13 Summary of the H₂/CO ratios

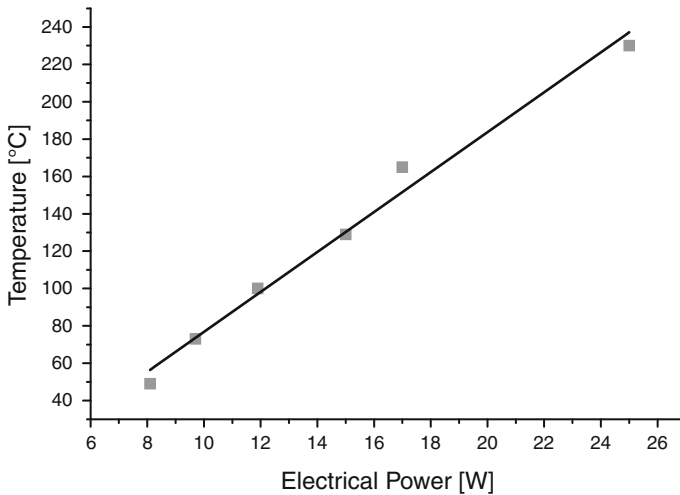


Fig. 14 Temperature of the catalyst for different electric heater powers

Effect of Temperature

Generally catalysts become active at higher temperature. Therefore, this feature was investigated by a catalyst heater. Figure 14 shows the temperature of the catalyst as a function of the electric heating power. The plasma power in all temperature experiments was 25 W so that the temperature effect of the plasma generation remains constant (and fairly low compared to the external heating). Figures 15 and 16 show that the formation of synthesis gas is a temperature dependent process.

Temperature increase with palladium as catalyst influences reduces the conversion of methane from 18 to 16%, as the conversion of carbon dioxide decreases from 11 to 9% (see

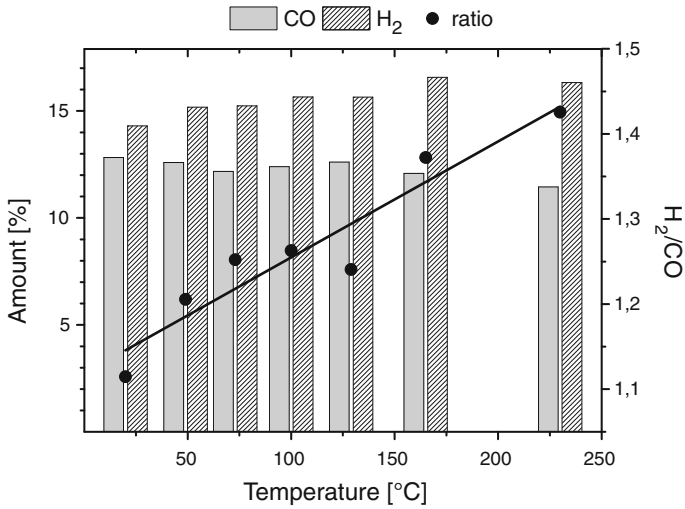


Fig. 15 Produced amount of the synthesis gas components (*left y-axis*) and its ratio (*right y-axis*) at various temperatures of the Pd/Al₂O₃ catalyst

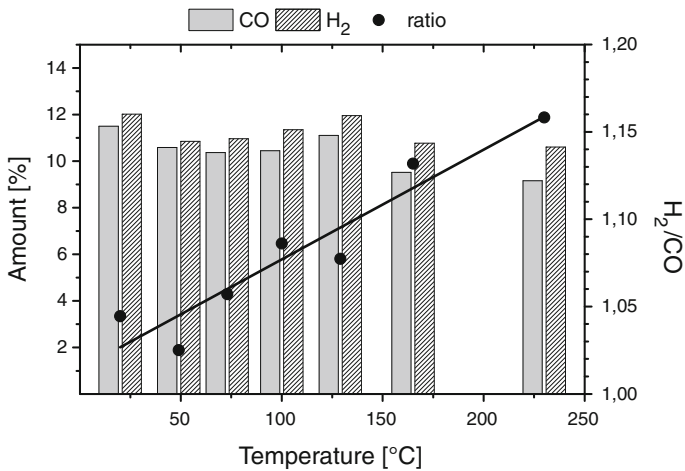


Fig. 16 Produced amount of H₂ and CO (*left y-axis*) and its ratio (*right y-axis*) at various temperatures of the Cu/Al₂O₃ catalyst

Fig. 17). Consequently the amount of carbon monoxide decreases from 13 to 12% (see Fig. 15). The reduction of both conversion efficiencies are based on volume expansion of the gas stream. This results in a shorter residence time and leads to the observations mentioned above. Additionally the amount of hydrogen increases from 14 to 17%. In this way an increase of the H₂/CO ratio from 1.1 to 1.4 can be observed.

The influence of the temperature using the copper catalyst was small in contrast to the palladium catalyst (see Figs. 16,18). The palladium catalyst activates the formation of hydrogen and deactivates the formation of carbon monoxide (see Fig. 15).

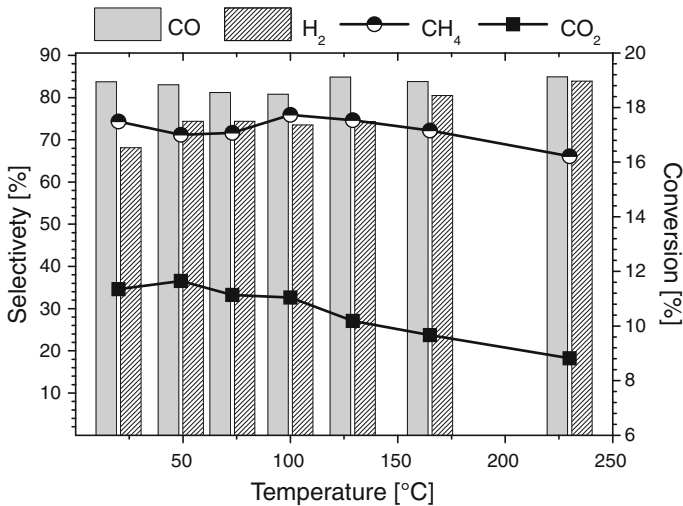


Fig. 17 Conversion of CH₄ and CO₂ (left y-axis) and selectivity (right y-axis) at various temperatures of the Pd/Al₂O₃ catalyst

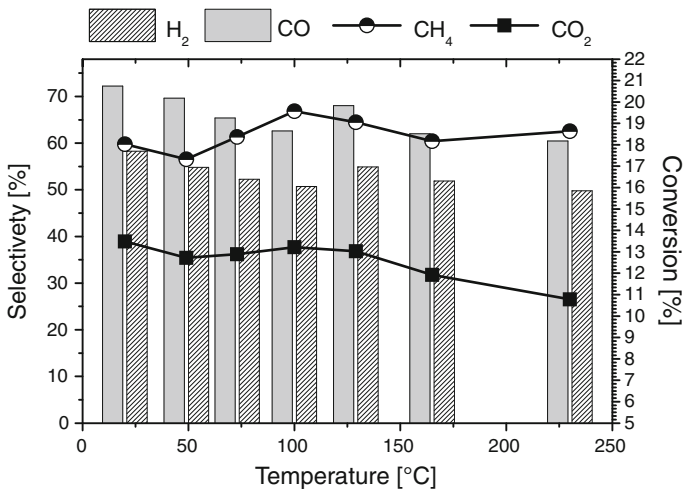


Fig. 18 Conversion of the starting material (left y-axis) and selectivity (right y-axis) at various temperatures of the Cu/Al₂O₃ catalyst

Higher temperatures significantly influence chemisorptions and solidity ratio of the palladium catalyst. Therefore, (7), (8) and (12) become more important.

Conclusion

The plug flow reactor supported by 13.56 MHz DBD is a useful tool to convert a mixture of methane and carbon dioxide into synthesis gas (H₂/CO). A gas mixture similar to the common biogas composition (60% methane and 40% carbon dioxide) was chosen. The

measurements comprise a homogenous dielectric barrier discharge reactor and a fluidized bed reactor supported by a DBD at low pressure. The power of the plasma was varied between 20 and 50 W. Furthermore the influence of the catalyst temperature was investigated between 25 and 250°C at a mild plasma power (25 W). The study includes yield, selectivity and ratio of hydrogen and carbon monoxide, as well as conversion of methane and carbon dioxide. A homogenous system (catalyst free) was used as a reference and a heterogeneous system (fluidized bed system) with two kinds of catalysts (palladium on aluminum oxide and copper on aluminum oxide) was used to test the activity of catalysts. Both catalysts change the product composition significantly. Under homogenous conditions the maximum synthesis gas ratio (H_2/CO) was 1.3, whereas the highest ratio is found with the fluidized Cu/Al_2O_3 catalyst (up to 1.7). Interestingly the highest yield and selectivity of hydrogen is found with the fluidized Pd/Al_2O_3 catalyst (the synthesis gas ratio was up to 1.7). The catalyst temperature had an influence on the synthesis gas ratio as well, but not as significant as the plasma power. Carbon black production starts at 40 W following an exponential trend (at lower power no carbon black is observed), and amounted to between 1 and 2%. A series of measurement indicates that the source of carbon black is methane exclusively.

Acknowledgments This project is part of the framework of the European Research Area (ERA) Chemistry call. The work was financially supported by the Deutsche Forschungs-Gesellschaft (DFG). Support by the Braunschweig *International Graduate School of Metrology* (IGSM) is gratefully acknowledged.

References

1. Metzger JO (2006) Produktion von flüssigen Kohlenwasserstoffen aus Biomasse. *Angew Chem* 118:710–713
2. Edwards JH, Maitra AM (1995) The chemistry of methane reforming with carbon dioxide and its current and potential applications. *Fuel Process Technol* 42:269–289
3. Bharadwaj SS, Schmidt LD (1995) Catalytic partial oxidation of natural gas to syngas. *Fuel Process Technol* 42:109–127
4. Tomishige K (2004) Syngas production from methane reforming with CO_2/H_2O and O_2 over NiO–MgO solid solution catalyst in fluidized bed reactors. *Catal Today* 89:405–418
5. Zhang K, Kogelschatz U, Eliasson B (2001) Conversion of greenhouse gases to synthesis gas and higher hydrocarbons. *Energy Fuels* 15:395–402
6. Zhou LM, Xue B, Kogelschatz U, Eliasson B (1998) Nonequilibrium plasma reforming of greenhouse gases to synthesis gas. *Energy Fuels* 12:1191–1199
7. Li M, Tian Y, Xu G (2007) Characteristics of carbon dioxide reforming of methane via alternating current (AC) corona plasma reactions. *Energy Fuels* 21:2335–2339
8. Longa H, Shanga S, Taob X, Yinb Y, Dai X (2008) CO_2 reforming of CH_4 by combination of cold plasma jet and Ni/g- Al_2O_3 catalyst. *Int J Hydrogen Energy* 33:5510–5515
9. Tao X, Qi F, Yin Y, Dai X (2008) CO_2 reforming of CH_4 by combination of thermal plasma and catalyst. *Int J Hydrogen Energy* 33:1262–1265
10. Zhang K, Eliasson B, Kogelschatz U (2002) Direct conversion of greenhouse gases to synthesis gas and C_4 hydrocarbons over zeolite HY promoted by a dielectric-barrier discharge. *Ind Eng Chem Res* 41:1462–1468
11. Eliasson B, Liu C, Kogelschatz U (2000) Direct conversion of methane and carbon dioxide to higher hydrocarbons using catalytic dielectric-barrier discharges with zeolites. *Ind Eng Chem Res* 39:1221–1227
12. Guoa F, Chua W, Xub J, Zhonga L (2008) Glow discharge plasma-assisted preparation of nickel-based catalyst for carbon dioxide reforming of methane. *Chin J Chem Phys* 21:481–486
13. Bo Z, Yan J, Li X, Chi Y, Cen K (2008) Plasma assisted dry methane reforming using gliding arc gas discharge: effect of feed gases proportion. *Int J Hydrogen Energy* 33:5545–5553
14. Kim SC, Chun YN (2008) Production of hydrogen by partial oxidation with thermal plasma. *Renewable Energy* 33:1564–1569

15. Rueangjitt N, Sreethawong T, Chavadej S (2008) Reforming of CO₂-containing natural gas using an AC gliding arc system: effects of operational parameters and oxygen addition in feed. *Plasma Chem Plasma Process* 28:49–67
16. Ghorbanzadeh AM, Modarresi H (2007) Carbon dioxide reforming of methane by pulsed glow discharge at atmospheric pressure: the effect of pulse compression. *J Appl Phys* 101:123303
17. Li D, Li X, Bai M, Tao X, Shang S, Dai X, Yin Y (2009) CO₂ reforming of CH₄ by atmospheric pressure glow discharge plasma: a high conversion ability. *Int J Hydrogen Energy* 34:308–313
18. Tomishige K, Asadullah M, Kunimori K (2004) Syngas production by biomass gasification using Rh/CeO₂/SiO₂ catalysts and fluidized bed reactor. *Catal Today* 89:389–403
19. Chun NY, Song HW, Kim SC, Lim MS (2008) Hydrogen-rich gas production from biogas reforming using plasmatron. *Energy Fuels* 22:123–127
20. Goujard V, Tatibouet JM, Batiot-Dupeyrat C (2009) Use of a non-thermal plasma for the production of synthesis gas from biogas. *Appl Catal A* 353:228–235
21. Rasi S, Veijanen A, Rintala J (2007) Trace compounds of biogas from different biogas production plants. *Energy* 32:1375–1380
22. Khoiyangbam RS, Kumar S, Jain MC, Gupta N, Kumar A, Kumar V (2004) Methane emission from fixed dome biogas plants in hilly and plain regions of northern India. *Bioresour Technol* 95:35–39
23. Kroker T, Kolb T, Krawczyk K, Młotek M, Schenk A, Schmidt-Szałowski K, Gericke KH (2009) Catalytic conversion of biogas in a fluidised bed reactor supported by a DBD. *Adv Appl Plasma Sci* 7:187–190
24. Sentek J, Krawczyk K, Młotek M, Kalczewska M, Kroker T, Kolb T, Schenk A, Gericke KH, Schmidt-Szałowski K (2010) Plasma-catalytic methane conversion with carbon dioxide in dielectric barrier discharges. *Appl Catal B* 94:19–26
25. Młotek M, Sentek J, Krawczyk K, Schmidt-Szałowski K (2009) The hybrid plasma-catalytic process for non-oxidative methane coupling to ethylene and ethane. *Appl Catal A* 366:232–241
26. Tsang W, Hampson RF (1986) Chemical kinetic data base for combustion chemistry, part I, methane and related components. *J Phys Chem Ref Data* 15:1087–1222
27. Darwent BB (1970) Bond dissociation energies in simple molecules. NBSDS-NBS 31
28. Pozzo M, Alfe D (2009) Hydrogen dissociation and diffusion on transition metal ([Ti, Zr, V, Fe, Ru, Co, Rh, Ni, Pd, Cu, Ag]-doped Mg(0001) surfaces. *Int J Hydrogen Energy* 34:1922–1930